

# Comparison of Macitentan and Bosentan on Right Ventricular Remodeling in a Rat Model of Non-vasoreactive Pulmonary Hypertension

Marc Iglarz, PharmD, PhD,\* Kyle Landskroner, PhD,\* Yasmina Bauer, PhD,\*  
Magali Vercauteren, PhD,\* Markus Rey,\* Berengère Renault, MSc,\* Rolf Studer, PhD,\*  
Enrico Vezzali, PhD,\* Diego Freti,\* Hakim Hadana,\* Manuela Schläpfer,\* Christophe Cattaneo,\*  
Céline Bortolamiol, MSc,\* Edgar Weber, PhD,\* Brian R. Whitby,† Stéphane Delahaye,\* Daniel Wanner,\*  
Pauline Steiner, MSc,\* Oliver Naylor, PhD,\* Patrick Hess,\* and Martine Clozel, MD\*

**Aims:** We compared the efficacy of macitentan, a novel dual endothelin A/endothelin B receptor antagonist, with that of another dual endothelin receptor antagonist, bosentan, in a rat model of non-vasoreactive pulmonary hypertension (PH) with particular emphasis on right ventricular (RV) remodeling.

**Methods and Results:** Unlike monocrotaline or hypoxic/sugen rats, bleomycin-treated rats presented a non-vasoreactive PH characterized by the absence of pulmonary dilatation to adenosine. We therefore chose the bleomycin rat model to compare the effects of the maximally effective doses of macitentan and bosentan on pulmonary vascular and RV remodeling. Macitentan ( $100 \text{ mg} \cdot \text{kg}^{-1} \cdot \text{d}^{-1}$ ), but not bosentan ( $300 \text{ mg} \cdot \text{kg}^{-1} \cdot \text{d}^{-1}$ ), significantly prevented pulmonary vascular remodeling, RV hypertrophy, and cardiomyocyte diameter increase. Cardiac protection by macitentan was associated with a significant attenuation of genes related to cell hypertrophy and extracellular matrix remodeling. Microautoradiography and high performance liquid chromatography analysis showed greater distribution of macitentan than bosentan in the RV and pulmonary tissue.

**Conclusions:** Macitentan was more efficacious than bosentan in preventing the development of pulmonary and RV hypertrophies in a model of non-vasoreactive PH. Greater ability to distribute into the

tissue could contribute to the greater structural improvement by macitentan compared with bosentan.

**Key Words:** macitentan, bosentan, pulmonary hypertension, endothelin, right ventricle

(*J Cardiovasc Pharmacol*™ 2015;66:457–467)

## INTRODUCTION

Endothelins are vasoactive peptides of which endothelin-1 (ET-1) is the most abundant in the lung. ET-1 responses are mediated via activation of 2 homologous G protein-coupled receptor subtypes, endothelin A receptor (ET<sub>A</sub>) and endothelin B receptor (ET<sub>B</sub>). Beyond its vasoconstrictive action, ET-1 is involved in deleterious processes affecting vascular and organ remodeling, such as hypertrophy, fibrosis, and inflammation.<sup>1</sup> Organ-selective upregulation of the ET system in cardiovascular diseases, including pulmonary hypertension (PH),<sup>2,3</sup> and its local autocrine/paracrine activity associated with a high tissue receptor density<sup>4,5</sup> suggest that the ET system can act as a key player on long-term disease progression by contributing to target organ remodeling. PH is a progressive disease leading to right ventricular (RV) failure and ultimately death, even on currently available therapy. ET receptor antagonism is an attractive approach to protect cardiac cells from hypertrophy as it provides, beyond direct inhibition of ET signaling, neurohormonal blockade. Indeed, ET receptor antagonists were shown to be sympatholytic and to decrease aldosterone levels in patients with heart failure.<sup>6</sup> The involvement of ET-1 in the pathophysiology of PH has been confirmed by the efficacy of first-generation ET receptor antagonists, which improved symptoms and delayed time to clinical worsening in patients with group 1 PH.<sup>7,8</sup> Recently, in the event-driven SERAPHIN trial, macitentan (10 mg) met its primary endpoint by significantly reducing the risk of morbidity and mortality by 45% in these patients.<sup>9</sup>

Macitentan is a novel dual ET<sub>A</sub> and ET<sub>B</sub> receptor antagonist with physicochemical properties favoring sustained receptor binding and high tissue distribution.<sup>10,11</sup> It was selected for development based on its oral efficacy in vivo in animal models of systemic and PH.<sup>11–13</sup> In the monocrotaline-treated rat model of PH, macitentan dose

Received for publication January 5, 2015; accepted July 2, 2015.

From the \*Drug Discovery Department, Actelion Pharmaceuticals Ltd, Allschwil, Switzerland; and †Covance Laboratories Ltd, Harrogate, North Yorkshire, England.

All authors except B. R. Whitby are employees of Actelion Pharmaceuticals Ltd. Dr. Landskroner is now with Novartis AG, Basel, Switzerland. The remaining authors report no conflicts of interest.

Supplemental digital content is available for this article. Direct URL citations appear in the printed text and are provided in the HTML and PDF versions of this article on the journal's Web site ([www.jcvp.org](http://www.jcvp.org)).

Reprints: Marc Iglarz, PharmD, PhD, Drug Discovery Department, Actelion Pharmaceuticals Ltd, Gewerbestrasse 16, CH-4123 Allschwil, Switzerland (e-mail: [marc.iglarz@actelion.com](mailto:marc.iglarz@actelion.com)).

Copyright © 2015 Wolters Kluwer Health, Inc. All rights reserved. This is an open access article distributed under the terms of the Creative Commons Attribution-NonCommercial-NoDerivatives License 4.0 (CC BY-NC-ND), which permits downloading and sharing the work provided it is properly cited. The work cannot be changed in any way or used commercially.

dependently prevented the development of PH, decreased RV hypertrophy, and increased survival.<sup>11</sup>

PH patients who respond acutely to vasodilators (ie, vasoreactive PH) represent a form of disease associated with exaggerated pulmonary vasoconstriction and/or at an early stage of the disease before development of established vascular lesions because of remodeling. These patients are amenable for long-term treatment with calcium channel antagonists, whereas nonresponders (ie, non-vasoreactive PH) are considered for other pharmacological options: phosphodiesterase type 5 inhibitors, ET receptor antagonists, prostacyclin receptor agonists, or guanylyl cyclase activators.<sup>14</sup> In non-vasoreactive PH, vascular remodeling associated with cell proliferation contributes to the maintenance of elevated pulmonary vascular resistance leading to RV remodeling and ultimately to a decompensated heart failure. Therefore, to compare the efficacy of macitentan versus another dual ET receptor antagonist, bosentan, on RV remodeling, we searched for a model of non-vasoreactive PH to focus on anti-remodeling effects beyond pulmonary vasodilation. The question whether animal models reflect vasoreactive or non-vasoreactive PH remains unknown. In this study, we first screened several PH rat models for acute response to vasodilators and then compared the disease-modifying efficacy of macitentan and bosentan with particular emphasis on RV remodeling.

## MATERIALS AND METHODS

### Animals and Characterization of the Non-vasoreactive PH Bleomycin Rat Model

This study was conducted in accordance with both Swiss Animal Protection Laws and Directive 2010/63/EU of the European Parliament on the protection of animals under scientific purposes and was specifically approved by Basellandschaft Cantonal Veterinary Office under license 371. Male Wistar rats (180–220 g body weight) were purchased from Harlan Laboratories B.V. (Venray, NL). All animals were housed in climate-controlled conditions with 12 hours of light/dark, maintained under identical conditions, and had free access to normal pelleted rat chow and drinking water. Saline or bleomycin was instilled through an intratracheal microsyringe (Model IA-1B-R; Penn-Century Inc, Wyndmoor, PA). Control animals received 1 mL/kg of sterile saline followed by 1 mL/kg of air. Bleomycin-treated rats received a single dose of sterile bleomycin sulfate (1.5 mg/kg) dissolved in 1 mL/kg of saline, also followed by 1 mL/kg of air to distribute the drug equally throughout the lungs. Generation of other animal models of PH and characterization of the presence or absence of vasoreactive PH are described in the **Supplemental Digital Content 1** (see **Supplementary Material S1**, <http://links.lww.com/JCVP/A207>).

### Measurements of Pulmonary Pressures in Bleomycin Rat Model by Means of Telemetry

Conscious rats were equipped with telemetry transmitters to measure mean pulmonary arterial pressure (mPAP) as previously described.<sup>15</sup> Briefly, rats were anesthetized by inhalation of 2.5% isoflurane and were mechanically ventilated. After abdominal laparotomy and right thoracotomy, the

transmitter was sutured into the abdominal cavity and the sensing catheter was positioned into the thorax via a trocar. The sensing catheter was then inserted into the RV and pushed into the pulmonary artery (PA). Tracings of the pulmonary signals were monitored continuously to verify the proper position in the PA during the surgery. The catheter was sutured onto the RV and the chest closed. During the surgery and throughout the next 5 days, rats received 0.03 mg/kg buprenorphine for analgesia. Seven to 9 days after instillation of bleomycin, rats developed PH and were orally treated with single doses of vehicle, macitentan, or bosentan and mPAP was measured.

### Study Design for Comparison of Macitentan Versus Bosentan Chronic Treatment

Rats were treated orally by gavage with vehicle (n = 18), 100 mg·kg<sup>-1</sup>·d<sup>-1</sup> macitentan (n = 18), or 300 mg·kg<sup>-1</sup>·d<sup>-1</sup> bosentan (n = 16) 1 day before intratracheal bleomycin instillation. Treatment was continued for 4 weeks. At the end of the study, rats underwent echocardiographic analysis and then were euthanized and organs were collected for assessment of RV hypertrophy and lung morphometric analysis, as described below.

### RV Hypertrophy and Echocardiography

Transthoracic 2D, M-mode, and Doppler imaging were performed in 8 animals per group using a Vivid 7 Ultrasound (GE Healthcare, Aurora, OH) echograph with linear and sectorial probes operated at 14 and 10 MHz, respectively, and data were analyzed using Echopac PC software. Animals were examined 28 days post-bleomycin instillation under isofluran-induced narcosis (2.5%, inhalation). Measurements, performed by 2 sonographers blinded to the treatment groups, were made in accordance with the conventions of the American Society of Echocardiography. M-mode measurements of RV free wall thickness and end-diastolic cavity dimension (left ventricle: LV and RV areas) were measured in the parasternal short axis view, just below the level of the aortic valve, and their ratio was calculated. Pulsed wave Doppler of pulmonary outflow was recorded in the parasternal short axis view at the level of the aortic valve. The sample volume was placed proximal to the pulmonary valve leaflets and aligned to maximize laminar flow. In addition, the PA acceleration time, velocity time integral, and ejection time (ET) were measured. By combining PA velocity time integral, PA area, and heart rate, echographic cardiac output was determined. The tricuspid valve was also evaluated for the presence of tricuspid regurgitation with color and continuous-wave Doppler in the apical 4-chamber view; no alteration was detected. At the time of killing, that is, after echocardiography, a rapid excision of the lungs and heart was performed through a ventral thoracotomy, and each organ was weighed. After removal of the atria to the plane of the atrial-ventricular valves, the RV free wall was dissected from the LV and septum. The RV and LV + septum were weighed, and the RV-to-LV + septum ratio (Fulton index) was calculated. Tibia lengths were measured to normalize read outs because animals presented body weight differences between the groups at the end of study. Eight RVs from each group were then processed for

quantitative polymerase chain reaction, whereas the remaining samples were used for histological analysis.

## Histology and Morphometry

Pulmonary arterial wall thickness measurement was adapted from Mouchaers et al<sup>16</sup> to assess pulmonary vascular hypertrophy. Lungs (left lobe) and hearts (RV) were cut sagittally, fixed in 10% neutral buffered formalin solution (4% formaldehyde), embedded in paraffin, sectioned at 4  $\mu\text{m}$ , and stained with hematoxylin–eosin, sirius red, and Orcein (lungs only). Slides were examined with Olympus BX46 microscope, DP25 digital camera, and CellSens Standard software version 1.3 (Olympus Corporation, Tokyo, Japan). For each group, 24 transversely cut muscular pulmonary arterioles, ranging from 15 to 100  $\mu\text{m}$  in diameter, were randomly selected, depicted at high-power field (objective  $\times 40$ ), and measured in a blinded fashion. The internal lamina elastic was considered as inner perimeter; therefore, the real caliber was extrapolated independently from the contraction status of the arteries, and then the relative pulmonary arterial wall thickness (RPAWT) was calculated as follows:

$$\text{RPAWT} = \text{medial wall thickness} / \text{outer radius.}$$

$$\text{Medial wall thickness} = \text{outer radius} - \text{inner radius.}$$

$$\text{Outer radius} = \sqrt{(\text{outer area} / \pi)}.$$

$$\text{Inner radius} = \text{inner perimeter} / 2\pi.$$

Mean values per animal and then per group were calculated.

Cardiomyocyte diameter was measured using a method adapted from Henkens et al<sup>17</sup> to assess cardiomyocyte hypertrophy. For each animal, 40 transversely cut cardiomyocytes, taken from areas not affected by cardiomyopathy, were randomly selected, depicted at medium power fields (objective  $\times 20$ ), and analyzed in a blinded fashion. Cardiomyocyte diameters, chosen parallel to minimize the standard error at selection, were measured in microns. Mean values per animal and then per group were calculated.

## Vascular Reactivity

Left PAs (2 mm in length) were mounted in organ baths under isometric conditions and bubbled with the following gas mixture: 5% CO<sub>2</sub>, 16% O<sub>2</sub>, and 79% N<sub>2</sub>. After a recovery period, vessels were stretched (2  $\times$  0.5 g) and depolarized twice with 60 mM KCl. Endothelium-dependent relaxations were obtained with cumulative doses of acetylcholine (10<sup>-9</sup> to 10<sup>-5</sup> M) after precontraction with norepinephrine corresponding to approximately 80% of the contraction to 60 mM KCl. After a 45-minute recovery period, endothelium-independent relaxations were achieved with cumulative doses of sodium nitroprusside (10<sup>-10</sup> to 10<sup>-6</sup> M). After another 45-minute recovery period, 10  $\mu\text{M}$  serotonin was applied to the vessel.

## Gene Expression

Right heart ventricles (8 animals per group) were collected in RNAlater (Ambion, Austin, TX). Total RNA was isolated using MagMAX 96 kit (AM1839; Ambion)

according to the manufacturer's instructions or the RNeasy mini fibrous tissue kit, including the DNAase treatment according to the manufacturer's protocol (QIAGEN, Hilden, Germany). The quantity of RNA was measured using a Nanodrop spectrophotometer (Thermo Fisher, Suwanee, GA), and RNA quality was assessed using a Bioanalyzer 2100 (Agilent, Santa Clara, CA). Total RNA was reverse transcribed with the high-capacity complementary DNA archive kit and subsequently preamplified using the TaqMan PreAmp Master Mix according to the manufacturer's protocols (Applied Biosystems, Carlsbad, CA) and quantified in real time using an ABI PRISM 7900 Sequence Detection System (Applied Biosystems/Life Technologies, Carlsbad, CA) or a BIOMARK HD system (Fluidigm, San Francisco, CA). The following commercial TaqMan assays from Applied Biosystems were used for messenger RNA detection: Coll1a1 Rn01463848\_m1, Fn1 Rn00569575\_m1, Lgals3 Rn00582910\_m1, Lox Rn00566984\_m1, Nppa Rn00664637\_g1, Nppb Rn00676450\_g1, Timp1 Rn01430873\_g1, Fst Rn00561225\_m1, and Inhba Rn01538592\_m1; and for normalization: Ppia Rn00690933\_m1, Pgl1 Rn00821429\_g1, and Hprt1 Rn01527840 for the Fluidigm platform or B2m Rn00560865\_m1, Gusb Rn00566655\_m1, Ppia Rn00690933\_m1, Ppib Rn003302274\_m1, Rock1 Rn00579490\_m1, and Tor2a Rn04218104\_m1 for analysis on ABI PRISM 7900. Results were calculated using the delta Ct method and expressed as fold changes between treated and vehicle animals.

## Lung Microautoradiography Study

Nineteen days after bleomycin or saline instillation, rats were administered a single oral dose of 3 mg/kg radiolabeled <sup>14</sup>C-macitentan (240 mCi/kg) or 15 mg/kg <sup>14</sup>C-bosentan (585 mCi/kg) and were euthanized under isoflurane-induced narcosis (2.5%, inhalation) at a time point corresponding to the respective plasma T<sub>max</sub> of the compounds (ie, 8 hours for macitentan and 2 hours for bosentan) and T<sub>max</sub> + 6 hours. These doses were selected based on their ability to reach similar plasma concentrations of the drug at T<sub>max</sub>. After perfusion of the lung with saline, right middle lobe sections from each animal were cut into small pieces and frozen in isopentane precooled with dry ice and processed for microautoradiography. For structure identification, hematoxylin and eosin or modified Masson's trichrome co-staining was used with the following procedure: samples were placed in a cryo-microtome (Leica CM3050; Leica, Nussloch, Germany) and replicate 5  $\mu\text{m}$  sections cut. These sections were thaw mounted onto microscope slides that were pre-coated with nuclear photographic emulsion. Radioactive carbon-14 standards were also prepared in water in the nominal ranges of 0.093–555 kBq/g. These standards were freeze embedded and cryosectioned in a similar manner to the lung tissues described above. After autoradiographic exposure for 67 days, the slides were photographically processed and histologically evaluated.

## Pulmonary and Cardiac Drug Concentrations

The pharmacokinetic study of drug concentrations in lung and RV was performed in separate animals. Nineteen days after bleomycin instillation, rats (n = 6 per group) were



acutely treated by oral gavage with either macitentan (3 mg/kg) or bosentan (15 mg/kg). These doses were identical to those used in the microautoradiography study. At the respective  $T_{max}$  of each drug, sublingual vein blood was collected under isoflurane anesthesia. At  $T_{max} + 6$  hours of each drug, all rats were anesthetized under isoflurane-induced narcosis (2.5%, inhalation) and killed by retrograde perfusion via the abdominal aorta (perfusion pressure, 90 mm Hg), with a pre-warmed phosphate buffer solution. The vena cava was dissected to prevent the recirculation of perfusate. After perfusion, the lung and RV were harvested, dissected, weighed, snap frozen, and stored at  $-80^{\circ}\text{C}$ . Plasma and organ concentrations of macitentan, its active metabolite ACT-132577, and bosentan were measured by liquid chromatography coupled to mass spectrometry (LC-MS), as previously described.<sup>11</sup> A similar study using the same doses of drugs was performed in monocrotaline rats (see **Supplementary Material S1, Supplemental Digital Content**, <http://links.lww.com/JCVP/A207>, for animal preparation) to confirm

the pattern of distribution of macitentan and bosentan in another model of PH.

## Expression of Results and Statistical Analyses

Results are expressed as means  $\pm$  SEM. Analysis of variance for repeated measures followed by the Newman-Keuls procedure for multiple comparisons was used for between-group comparisons.

## RESULTS

### Evaluation of Vascular Reactivity and Search for a Non-vasoreactive PH Model

Rats treated with bleomycin or monocrotaline or animals receiving a single administration of Sugen 5416, combined with exposure of 3 weeks of chronic hypoxia (10%  $\text{O}_2$ ), followed by 2 weeks of reexposure to normoxia (SU/HYP), developed different grades of PH with increased mPAP of  $33 \pm 3$ ,  $52 \pm 6$ , and  $86 \pm 5$  mm Hg, respectively,

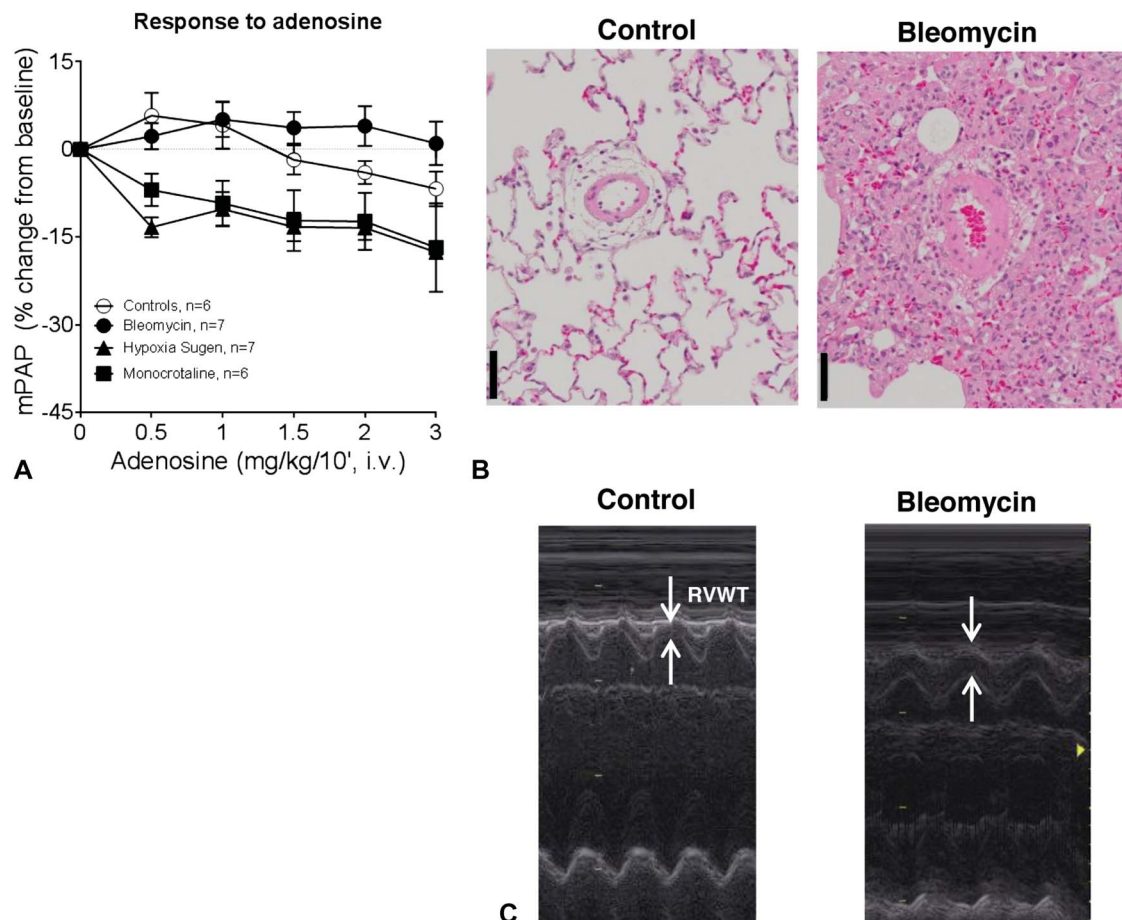


**FIGURE 1.** Characterization of the non-vasoreactive bleomycin-induced PH model. A, Dose–response curve for adenosine (intravenous) on mPAP in anesthetized rats without (controls) or with PH;  $n = 6$ – $7$  per group. B, Representative pictures of pulmonary arterial remodeling in control (left) and bleomycin-instilled rats (right). Hypertrophied pulmonary arterioles of bleomycin rats are surrounded by stromal changes, such as fibrotic foci and edema. Staining: hematoxylin and eosin (scale bar represents  $50 \mu\text{m}$ ). C, Representative M-mode measurements of RV free wall thickness (RVWT) as observed in the parasternal short axis view.

compared with an mPAP of  $21 \pm 1$  mm Hg in healthy control animals. Intravenous infusion of adenosine decreased pulmonary pressure by approximately 15% in monocrotaline and SU/HYP rats, but not in bleomycin-instilled rats (Fig. 1A), despite a lower baseline mPAP in this latter model. A similar response pattern was observed after acute amlodipine administration (data not shown). Therefore, the bleomycin-instilled rat was identified as a non-vasoreactive PH model. This PH model is not solely because of fibrotic lung disease as pathological vascular lesions in the lung of bleomycin rats recapitulate most of the lesions described in group 1 PH patients<sup>18</sup>: medial hypertrophy, intimal proliferative and fibrotic changes, and adventitial thickening with moderate perivascular inflammatory infiltrate (Fig. 1B). However, no complex or thrombotic lesions were found.

We next assessed the temporal development of bleomycin-induced PH in conscious freely moving rats that were implanted with telemetry pressure transmitters. As shown in Figure 2A, mPAP started to increase 2–3 days after intratracheal instillation of bleomycin, reaching a plateau of +13 mm Hg versus control rats at day 7, and this elevated mPAP level remained unchanged until day 28.

### Superior Long-term Efficacy of Macitentan in the Prevention of RV Remodeling

We next performed a dose–response experiment in bleomycin-treated rats to determine the maximal effective dose on mPAP (Fig. 2B). Maximal effective doses on pulmonary hemodynamics were selected to assess optimally the potential of each drug on vascular and cardiac remodeling. Although 10 and 30 mg/kg seemed to be the first maximal effective doses on hemodynamics for macitentan and bosentan, respectively, we decided to select 10 times higher doses to ensure a positive effect of remodeling. Therefore, the 100 mg/kg dose of macitentan was selected for a direct comparison study with bosentan, which was used at 300 mg/kg, as

this was previously shown to be the maximal effective dose on RV remodeling<sup>11</sup> and hemodynamics<sup>13</sup> in PH animal models.

In the absence of compound treatment, bleomycin-instilled rats displayed a marked decrease in body weight and a significant increase of RV free wall thickness versus saline-instilled control animals after 4 weeks (Table 1, Fig. 1C). However, bleomycin-instilled rats showed neither significant RV dysfunction, as assessed by echocardiography (Table 1), nor development of RV fibrosis (data not shown). RV remodeling in bleomycin-induced PH animals was characterized by a 51% increase of RV/(LV + S) ratio and a 14% increase of cardiomyocyte diameter compared with saline-instilled control animals (Figs. 3A, B). Bleomycin-induced lung fibrosis was observed (Fig. 1B) and pulmonary arterial walls thickened in bleomycin-treated animals by 53% relative to saline-instilled controls (Fig. 4). Both macitentan and bosentan consistently and significantly prevented body weight loss in bleomycin-instilled animals (both  $P < 0.01$  vs. bleomycin + vehicle) (Table 1). However, only macitentan consistently and significantly reduced the development of RV hypertrophy (Fulton index) and cardiomyocyte size increase, by 82% and 100%, respectively (both  $P < 0.01$  vs. bleomycin + vehicle, Figs. 3A, B), whereas bosentan, despite a tendency of decrease, had no significant effect. Macitentan, but not bosentan, significantly reduced pulmonary arterial wall thickening by  $-60%$  ( $P < 0.05$  vs. bleomycin + vehicle) (Figs. 4A, B). Both macitentan and bosentan partially prevented the development of lung fibrosis (data not shown).

### Macitentan Attenuates Bleomycin-induced RV Gene Expression Changes

To further characterize the better efficacy of macitentan in comparison with bosentan in the prevention of RV remodeling at a molecular level, gene expression analysis was performed on isolated right heart ventricles that were

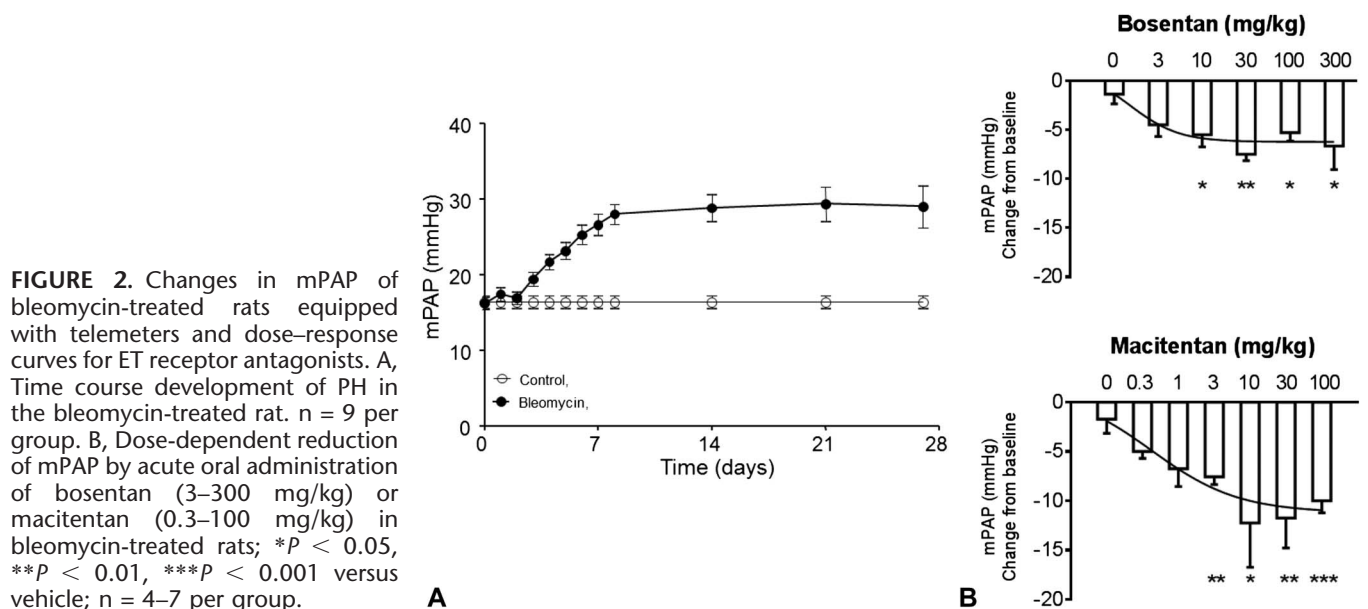


**TABLE 1.** Effect of 4-week Treatment With Macitentan (100 mg·kg<sup>-1</sup>·d<sup>-1</sup>), Bosentan (300 mg·kg<sup>-1</sup>·d<sup>-1</sup>), and Vehicle on Echocardiographic Parameters in Bleomycin-instilled Rats Versus Saline

	Saline	Bleomycin		
		Vehicle	Macitentan	Bosentan
Body weight (g)	318 ± 6	247 ± 18 <sup>+++</sup>	293 ± 7 <sup>**</sup>	298 ± 8 <sup>**</sup>
Heart rate (bpm)	412 ± 16	366 ± 18	404 ± 10	387 ± 11
PAAT/CL	0.15 ± 0.02	0.11 ± 0.01	0.13 ± 0.01	0.14 ± 0.01
PAAT/ET	0.27 ± 0.03	0.22 ± 0.02	0.22 ± 0.02	0.25 ± 0.01
PA VTI (cm)	5.04 ± 0.27	5.22 ± 0.67	5.69 ± 0.10	5.73 ± 0.21
RV CO (mL/min)	178 ± 7	157 ± 18	198 ± 10*	206 ± 10*
RV/LV areas	0.58 ± 0.04	0.67 ± 0.05	0.56 ± 0.03	0.61 ± 0.07
RVWT (mm)	0.67 ± 0.03	0.96 ± 0.12 <sup>+</sup>	0.74 ± 0.04	0.73 ± 0.08

All data are presented as means ± SEM. n = 8 rats per group.

<sup>+</sup>P < 0.05, <sup>+++</sup>P < 0.001 versus saline; \*P < 0.05, <sup>\*\*</sup>P < 0.01 versus bleomycin rats.

CL, cardiac length (ms); CO, cardiac output; ET, ejection time (ms); PAAT, PA acceleration time (ms); RVWT, RV free wall thickness; VTI, velocity time integral (ms).

isolated from compound-treated and vehicle-treated bleomycin-instilled animals or saline-instilled control animals. The genes that were used in this investigation were selected on the basis of known contribution in remodeling/extracellular matrix deposition, that is, collagen1a1 (*Coll1a1*), fibronectin (*Fn1*), lysyl oxidase (*Lox*), tissue inhibitor of metalloproteinase 1 (*Timp1*), follistatin (*Fst*), inhibin A (*Inhba*), and galectin-3 (*Lgals3*), or cardiac function, that is, natriuretic peptide A (*Nppa*) and natriuretic peptide B (*Nppb*). Gene expression analysis revealed that macitentan normalized the expression of all investigated genes, in the case of natriuretic peptide A (*Nppa*) even to baseline (Fig. 5), whereas bosentan, despite a tendency of decrease, had no significant effect on bleomycin-induced gene expression changes with the exception of fibronectin 1 (*Fn1*) and galectin-3 (*Lgals3*). Therefore, at the level of gene expression normalization in the RV, macitentan also showed superiority in comparison with bosentan.

### Efficacy on Smooth Muscle Cell Dysfunction

Vascular reactivity was tested in left PAs, which were isolated after 4 weeks from compound-treated and vehicle-

treated bleomycin-instilled animals or saline-instilled control animals, using organ baths under isometric conditions. In vessels from bleomycin-instilled rats, no obvious endothelial dysfunction was observed in response to acetylcholine but smooth muscle cell dysfunction was suggested by the rightward shift (although nonsignificant) of the response to sodium nitroprusside and the significantly increased response to serotonin (5-HT) (Figs. 6A, B, C). Bosentan and macitentan partially reduced response to 5-HT to a similar extent (−58% and −62%, respectively, P < 0.05 vs. bleomycin + vehicle) (Fig. 6C), suggesting that both compounds had similar efficacy to preserve vascular reactivity.

### Increased Tissue Penetration of Macitentan Versus Bosentan

Based on our investigations described in the previous sections, only macitentan displayed significant prevention of RV and PA remodeling in bleomycin-induced PH model. We thus explored the possibility of different tissue penetration capacity as one of the possible contributors for the improved efficacy of macitentan. To this end, <sup>14</sup>C-labeled macitentan and bosentan were used to investigate the tissue penetration

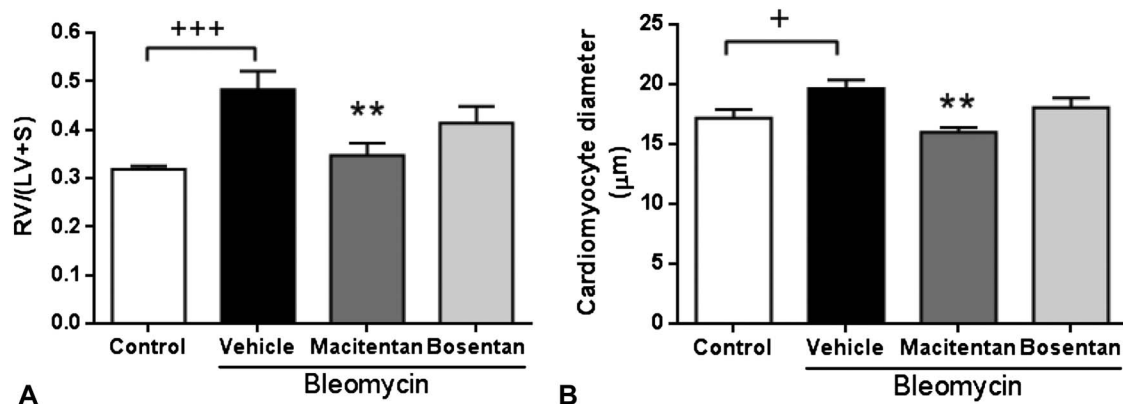


**FIGURE 3.** Effects of 4-week treatment with macitentan (100 mg·kg<sup>-1</sup>·d<sup>-1</sup>) and bosentan (300 mg·kg<sup>-1</sup>·d<sup>-1</sup>) in bleomycin-instilled rats. A, RV hypertrophy. B, RV cardiomyocyte size. <sup>+</sup>P < 0.05, <sup>+++</sup>P < 0.001 versus rats instilled with saline (control), <sup>\*\*</sup>P < 0.01 versus rats instilled with bleomycin and treated with vehicle; n = 8 per group.

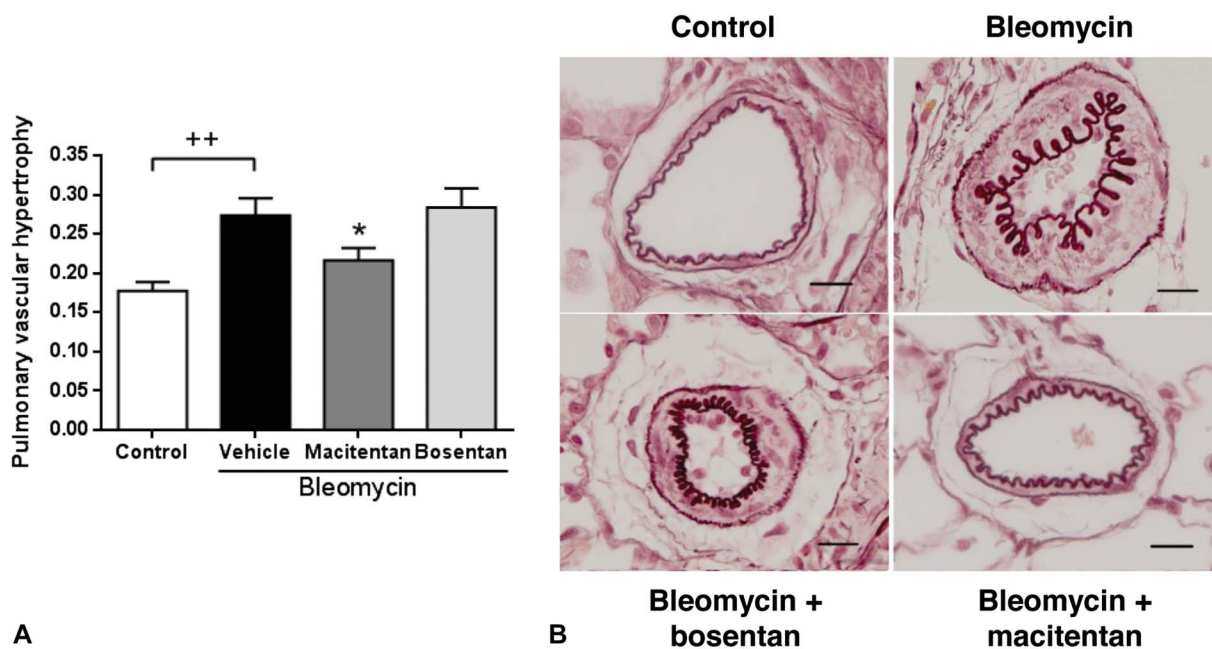


**FIGURE 4.** Effects of 4-week treatment with macitentan (100 mg·kg<sup>-1</sup>·d<sup>-1</sup>) or bosentan (300 mg·kg<sup>-1</sup>·d<sup>-1</sup>) on pulmonary arterial remodeling in bleomycin-instilled rats. **A**, Pulmonary arterial wall thickness; ++*P* < 0.01 versus rats instilled with saline (control), \**P* < 0.05 versus rats instilled with bleomycin and treated with; n = 16–18 per group. **B**, Representative pictures of PAs stained with Orcein, ×20 magnification (scale bar represents 20 μm).

properties of both compounds in vivo in lung and heart. Microautoradiography revealed that at T<sub>max</sub> after <sup>14</sup>C-drug administration, general lung tissue radioactivity was higher in rats treated with macitentan than with bosentan (Fig. 7A). For comparable plasma exposures, higher levels of radioactivity were present in the walls and the adventitia of the blood vessels in the cuboidal cells and in the smooth muscle/collagen region of the bronchioles of rats treated with macitentan, whereas in animals treated with bosentan, moderate levels of radioactivity were present in the same structures. At T<sub>max</sub> + 6 hours after drug administration, high levels of radioactivity were maintained in the general lung tissue of macitentan-treated rats, although the intensity was lower than at T<sub>max</sub> as observed in structures, such as cuboidal cells and blood vessels. In bosentan-treated rats, higher radioactivity was observed in the cuboidal cells and bronchiole smooth muscles compared with levels observed at T<sub>max</sub> (Fig. 7A), but general lung tissue radioactivity was lower in the bosentan-treated than in the macitentan-treated group. Of note, after single oral administration of radiolabeled macitentan, more radioactivity was apparent in the lung substructures, particularly the cuboidal cells and smooth muscle/collagen regions of the bronchioles, when the animals had been pretreated with bleomycin compared with control animals (Fig. 7B). Quantification of drug concentration by LC-MS in the lung at T<sub>max</sub> + 6 hours confirmed the microautoradiography findings as total lung contents of macitentan and its active major metabolite were approximately 4 times higher than that of bosentan for comparable plasma exposures as reflected by respective plasma concentrations at estimated T<sub>max</sub> (bosentan: 1625 ng/mL;

macitentan + metabolite: 2222 ng/mL). Moreover, the quantification of macitentan and its metabolite in the RV indicated a higher concentration than bosentan (Fig. 7C). This greater distribution of macitentan versus bosentan in lung and RV was confirmed in another model of PH (monocrotaline rats, Fig. 7C).

### DISCUSSION

Macitentan is a potent, novel dual ET receptor antagonist with superior in vivo pharmacological efficacy compared with existing ET receptor antagonists.<sup>12</sup> This was originally demonstrated by its remarkable activity in hypertensive rats after oral administration, in which macitentan achieved a superior blood pressure reduction compared with other ET receptor antagonists, such as ambrisentan and bosentan.<sup>11,12,19</sup> In the present study, using a rat model of non-vasoreactive PH, we demonstrated that macitentan has superior anti-remodeling effects on pulmonary arterial and RV hypertrophies than bosentan. In addition, macitentan showed higher RV and lung distribution than bosentan.

We conducted our studies in bleomycin-treated rats known to develop PH.<sup>20,21</sup> ET-1 and its receptors have been proposed to drive disease progression in this model.<sup>22–24</sup> Originally used as an antitumor agent, bleomycin is a glycopeptidic antibiotic known to induce pulmonary fibrosis through an early phase of epithelial/endothelial damage, followed by inflammation and ultimately fibrosis.<sup>25</sup> Although this model has been primarily used to investigate pulmonary fibrosis, the animals administered with bleomycin also develop PH<sup>20,21</sup>



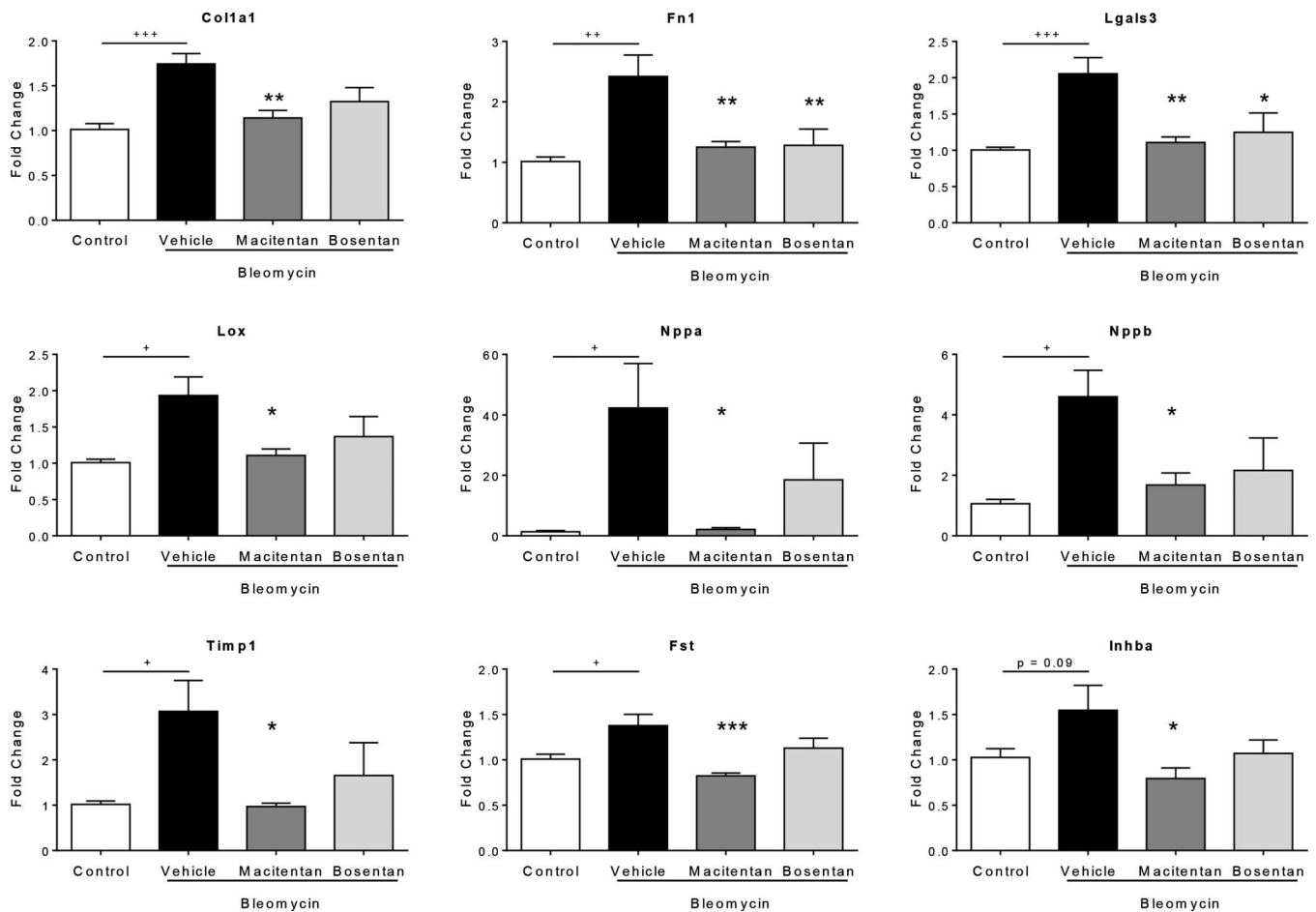


**FIGURE 5.** Effects of 4-week treatment with macitentan ( $100 \text{ mg} \cdot \text{kg}^{-1} \cdot \text{d}^{-1}$ ) and bosentan ( $300 \text{ mg} \cdot \text{kg}^{-1} \cdot \text{d}^{-1}$ ) on a panel of genes involved in RV remodeling.  $+P < 0.05$ ,  $++P < 0.01$ ,  $+++P < 0.001$  versus rats instilled with saline (control),  $*P < 0.05$ ,  $**P < 0.01$ ,  $***P < 0.001$  versus rats instilled with bleomycin and treated with vehicle;  $n = 8$  per group.

associated with epithelial activation of ET-1.<sup>23</sup> Unlike the monocrotaline rats that develop rapid progressive and transient PH leading to death, the bleomycin-treated rats develop moderate and sustained increase in pulmonary pressure, which makes it suitable to study compensatory mechanisms, such as RV hypertrophy.<sup>17,26,27</sup> We report here, for the first time, in conscious freely moving bleomycin-treated rats, the temporal development of pulmonary pressure elevation using telemetry. Although moderate when compared with other PH models, the increased mPAP remained elevated over the study period and was accompanied by mild RV hypertrophy with preserved function and pulmonary vascular hypertrophy. Unlike the monocrotaline and sugen/hypoxia rat models of PH, the bleomycin rat presented a non-vasoreactive PH characterized by the absence of an acute vasodilatory response to adenosine infusion and hypertrophic vascular remodeling.

To directly compare the differences of macitentan and bosentan in this novel model of non-vasoreactive PH, we aimed to use the highest efficacious dose of each compound. An off-target effect can be discarded as macitentan was shown to be selective for ET<sub>A</sub> and ET<sub>B</sub> receptors when screened at a concentration of  $10 \mu\text{M}$  in a panel of 63

radioligand binding assays.<sup>11</sup> Compared with the monocrotaline rat model in which both compounds were efficacious at lower doses,<sup>11</sup> the bleomycin rat model seemed less sensitive to ET receptor antagonism. This observation is confirmed by other studies demonstrating efficacy of bosentan on cardiac remodeling in hypoxic<sup>28</sup> and hypoxia/sugen<sup>29</sup> rats, whereas bosentan had no effect on this read out in our study. This suggests that the efficacy of compounds might be reduced in models on non-vasoreactive (eg, bleomycin) versus reactive PH (monocrotaline, hypoxia/sugen).

We recently presented evidence that macitentan had a greater pharmacological activity versus bosentan in vivo: in bleomycin-treated rats, the maximal efficacious dose of macitentan was able to further decrease mPAP when administered on top of the maximal efficacious dose of bosentan.<sup>13</sup> Together with the findings of the present study, showing a superiority of macitentan over bosentan on RV and pulmonary vessel remodeling, our data suggest that macitentan can achieve a more complete inhibition of the ET system in vivo. In addition to a longer effective half-life because of the presence of an active metabolite, macitentan differs from bosentan by its receptor-binding properties and its ability to



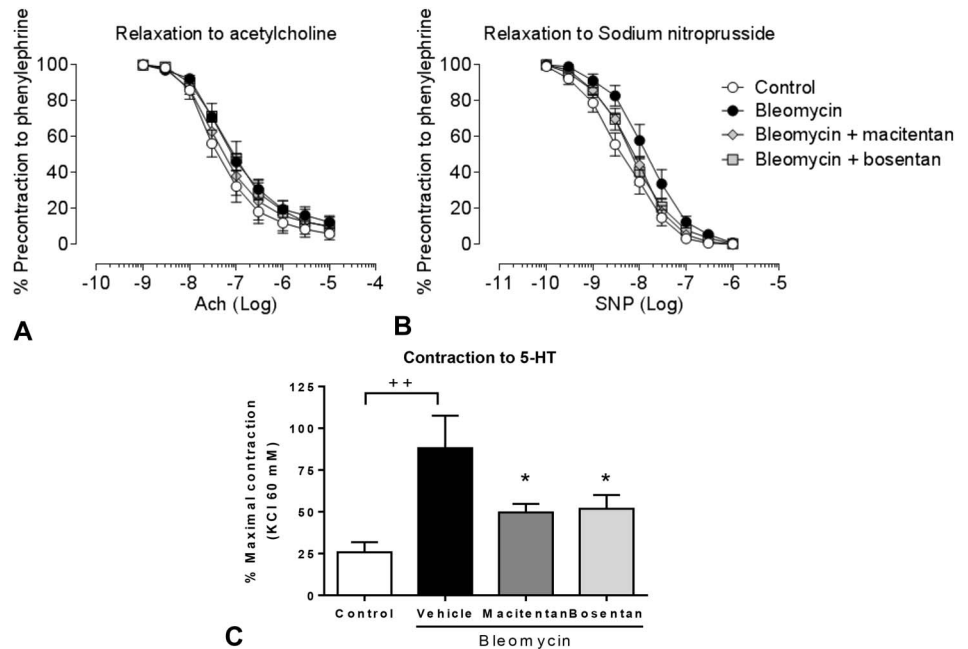


**FIGURE 6.** Effects of 4-week treatment with macitentan (100 mg·kg<sup>-1</sup>·d<sup>-1</sup>) or bosentan (300 mg·kg<sup>-1</sup>·d<sup>-1</sup>) on PA function. A, Dose–response curve to acetylcholine (ACh). B, Dose–response curve to sodium nitroprusside (SNP). C, Contraction to 10 μM serotonin (5-HT). ++*P* < 0.01 versus rats instilled with saline (control). \**P* < 0.05 versus rats instilled with bleomycin and treated with vehicle; n = 6–7 per group.

distribute into tissues. Macitentan is a competitive antagonist with a prolonged receptor occupancy half-life. Macitentan thus displays insurmountable antagonism, that is, it is capable of efficient receptor blockade irrespective of the ET-1 concentration.<sup>10,30</sup> In diseased tissues, where local ET-1 concentrations are elevated, such a binding mode together with the higher local concentration of the compound might confer superior blockade of downstream signaling induced by ET-1. In addition to the binding kinetics, we also hypothesized that macitentan could have differential tissue distribution compared with bosentan, which we thought could be because of differences in their physiochemical properties (eg, pKa, lipophilicity).<sup>11</sup> Using microautoradiography and tissue quantification by LC-MS, we were able to demonstrate (1) differential tissue distribution of macitentan in normal versus diseased lung and (2) increased lung and RV concentration of macitentan versus bosentan in 2 models of PH, suggesting that these findings are not limited to the bleomycin rat model but could apply to other models of PH. The use of radiolabeled material enabled us to study the distribution of both macitentan and its active metabolite. We previously reported that oral administration of macitentan leads to the formation of metabolite ACT-132577, a dual ET<sub>A</sub>/ET<sub>B</sub> antagonist. Although its overall potency on ET receptors is 5–10 times less than that of macitentan, ACT-132577 has a longer half-life than macitentan, accumulates with time, and is expected to contribute to the pharmacological effects observed after oral administration of macitentan.<sup>11,31</sup> The microautoradiography studies revealed increased distribution of macitentan-derived radioactivity in diseased lung tissue compared with healthy lungs. This latter observation, which might not be specific to macitentan and could apply to other ET receptor antagonists, may be because of an increased permeability of the damaged tissue and/or an upregulation of the ET binding sites in bleomycin rats.

Although macitentan showed greater effect on RV and pulmonary remodeling than bosentan, both drugs had similar efficacy on lung fibrosis. This discrepancy could be explained by 2 factors: first, as we used maximal effective doses of each compound to ensure maximal effect on the remodeling, one cannot rule out that a slight greater effect on mPAP obtained with macitentan (Fig. 2), possibly because of its ability to block more receptors than bosentan, could be responsible for its superior efficacy on RV and pulmonary remodeling compared with bosentan. Second, our results on lung fibrosis suggest that the ET system, although important, is not the sole driver in lung fibrosis and that a plateau effect has been reached with the 2 drugs. Of note, both clinical trials in patients with pulmonary fibrosis involving macitentan and bosentan did not reach their primary efficacy endpoints indicating that targeting the ET system alone may not be sufficient in this indication.

The superior efficacy of macitentan on RV remodeling, a known predictive marker of mortality,<sup>32</sup> associated with a greater distribution in the RV suggests that macitentan may have potential for superior long-term benefit on clinical outcome compared with bosentan. Although no clinical direct comparison was made, macitentan (10 mg) is currently the only ET receptor antagonist that demonstrated a dose-dependent effect on a composite hard endpoint (mortality/morbidity) in a clinical trial and a sustained 50% risk reduction in death or hospitalization because of PH during treatment.<sup>9</sup> In our study, RV protection was associated with a greater attenuation by macitentan of the expression of genes involved in extracellular matrix/cardiac remodeling (*Colla1*, *Lox*, *Timp1*). Expression of genes encoding mediators of fibrosis, such as fibronectin (*Fn1*)<sup>33</sup> and galectin-3 (*Lgal3*),<sup>34</sup> was similarly corrected by both drugs. In contrast to bosentan, macitentan significantly decreased *Inhba* and *Fst* genes. The *Inhba* gene encodes activin A, a homodimer of inhibin beta subunit, related

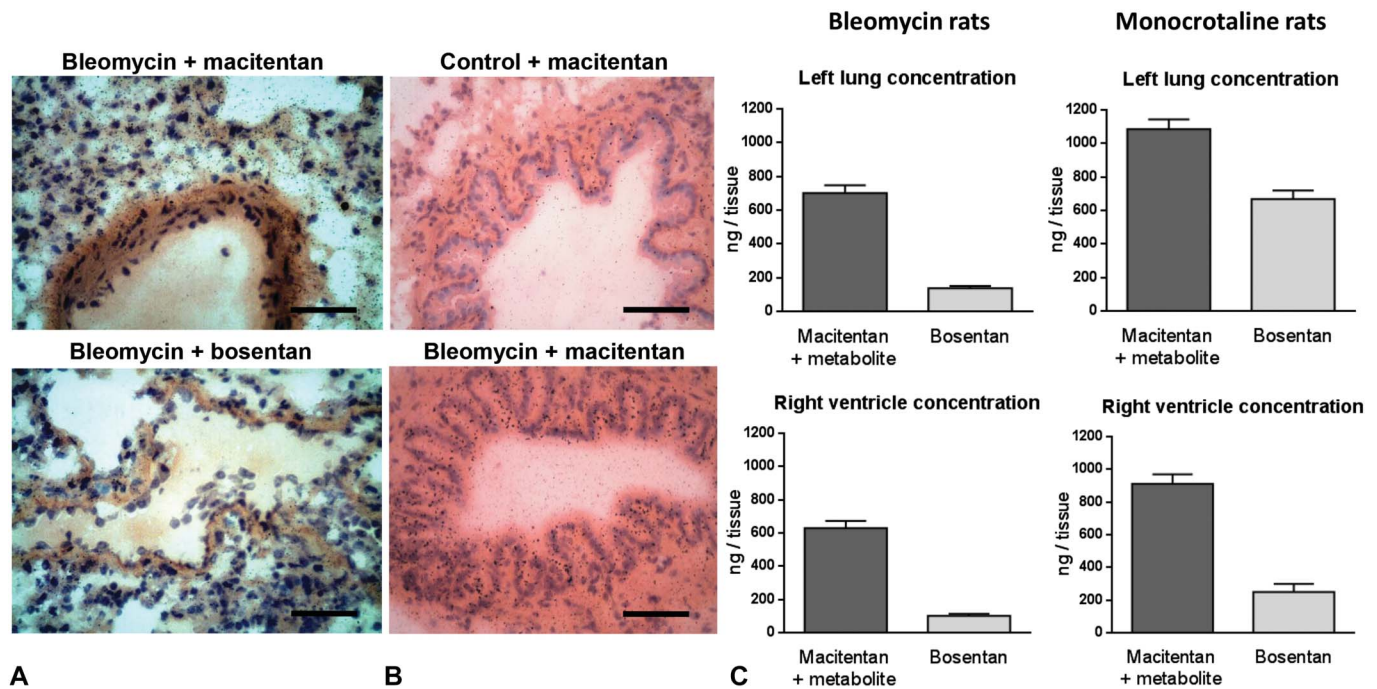


**FIGURE 7.** Tissue distribution and quantification of macitentan and bosentan in bleomycin rats. **A**, Microautoradiographs showing radioactivity (seen as silver grains) at respective  $T_{max}$  after oral administration of  $^{14}C$ -macitentan (top) and  $^{14}C$ -bosentan (bottom).  $^{14}C$ -Macitentan is able to reach more diffuse parenchymal lung distribution in bleomycin rats than  $^{14}C$ -bosentan. Staining: modified Masson's trichrome,  $\times 40$  magnification (scale bar represents  $20 \mu m$ ). **B**, Microautoradiographs showing radioactivity (seen as silver grains) of  $^{14}C$ -macitentan in the dissected lungs in control (top) and diseased bleomycin rat lungs (bottom). Staining: hematoxylin and eosin,  $\times 40$  magnification. **C**, Quantification by HPLC of drug concentrations in left lung (top) and right ventricle (bottom) at  $T_{max} + 6$  hours of bleomycin rats (left) and monocrotaline rats (right);  $n = 6$  per group.

to the transforming growth factor  $\beta$  superfamily and involved in cardiac remodeling and inflammation.<sup>35,36</sup> The *Fst* gene encodes follistatin, a negative regulator of activin that removes activin A from the circulation.<sup>37</sup> Follistatin is upregulated in patients with PH, and its plasma levels are correlated with increased mortality.<sup>38</sup> In our study, increase of follistatin was observed in parallel to activin A activation in bleomycin-treated rats, as a possible counterregulatory mechanism. Our data suggest that macitentan can blunt the activin A/follistatin axis to protect against the development of cardiac remodeling. Furthermore, the consistent and more pronounced attenuation of gene expression changes that are associated with heart remodeling could suggest improved local activity of macitentan in comparison with bosentan, also in the heart.

As a study limitation, we did not measure pulmonary pressures in bleomycin-instilled rats at the end of the chronic treatment with vehicle, macitentan, or bosentan. The reason for this is that, in contrast to telemetry, we could not detect an increase in mPAP in anesthetized bleomycin-instilled rats versus healthy animals probably because of an effect of anesthesia on hemodynamics.

In conclusion, our data show that the efficacy of macitentan is higher than that of bosentan in treating PH and RV hypertrophy in a rat model of non-vasoreactive PH induced by bleomycin. This may be because of the improvement of binding mode and pharmacokinetic profile (tissue distribution, long half-life). A more complete blockade of ET

receptors, achieved by macitentan, is a promising approach to treat diseases where local tissue ET-1 represents a significant component of the pathophysiology.

#### ACKNOWLEDGMENTS

We are grateful to Odette Birko, Eric Soubieux, and Aude Weigel for expert technical assistance.

#### REFERENCES

- Iglarz M, Clozel M. At the heart of tissue: endothelin system and end-organ damage. *Clin Sci (Lond)*. 2010;119:453–463.
- Dagassan PH, Breu V, Clozel M, et al. Up-regulation of endothelin-B receptors in atherosclerotic human coronary arteries. *J Cardiovasc Pharmacol*. 1996;27:147–153.
- Bauer M, Wilkens H, Langer F, et al. Selective upregulation of endothelin B receptor gene expression in severe pulmonary hypertension. *Circulation*. 2002;105:1034–1036.
- Desmarests J, Gresser O, Guedin D, et al. Interaction of endothelin-1 with cloned bovine ETA receptors: biochemical parameters and functional consequences. *Biochemistry*. 1996;35:14868–14875.
- Frelin C, Guedin D. Why are circulating concentrations of endothelin-1 so low? *Cardiovasc Res*. 1994;28:1613–1622.
- Sutsch G, Bertel O, Rickenbacher P, et al. Regulation of aldosterone secretion in patients with chronic congestive heart failure by endothelins. *Am J Cardiol*. 2000;85:973–976.
- Rubin LJ, Badesch DB, Barst RJ, et al. Bosentan therapy for pulmonary arterial hypertension. *N Engl J Med*. 2002;346:896–903.
- Galie N, Rubin L, Hoeper M, et al. Treatment of patients with mildly symptomatic pulmonary arterial hypertension with bosentan (EARLY

- study): a double-blind, randomised controlled trial. *Lancet*. 2008;371:2093–2100.
9. Pulido T, Adzerikho I, Channick RN, et al. Macitentan and morbidity and mortality in pulmonary arterial hypertension. *N Engl J Med*. 2013;369:809–818.
  10. Gatfield J, Mueller Grandjean C, Sasse T, et al. Slow receptor dissociation kinetics differentiate macitentan from other endothelin receptor antagonists in pulmonary arterial smooth muscle cells. *PLoS One*. 2012;7:e47662.
  11. Iglarz M, Binkert C, Morrison K, et al. Pharmacology of macitentan, an orally active tissue-targeting dual endothelin receptor antagonist. *J Pharmacol Exp Ther*. 2008;327:736–745.
  12. Bolli MH, Boss C, Binkert C, et al. The discovery of N-[5-(4-bromophenyl)-6-[2-[(5-bromo-2-pyrimidinyl)oxy]ethoxy]-4-pyrimidinyl]-N'-p ropylsulfamide (Macitentan), an orally active, potent dual endothelin receptor antagonist. *J Med Chem*. 2012;55:7849–7861.
  13. Iglarz M, Bossu A, Wanner D, et al. Comparison of pharmacological activity of macitentan and bosentan in preclinical models of systemic and pulmonary hypertension. *Life Sci*. 2014;118:333–339.
  14. Sitbon O, Humbert M, Jais X, et al. Long-term response to calcium channel blockers in idiopathic pulmonary arterial hypertension. *Circulation*. 2005;111:3105–3111.
  15. Rey M, Weber EW, Hess PD. Simultaneous pulmonary and systemic blood pressure and ECG interval measurement in conscious, freely moving rats. *J Am Assoc Lab Anim Sci*. 2012;51:231–238.
  16. Mouchaers KT, Schaliij I, de Boer MA, et al. Fasudil reduces monocrotaline-induced pulmonary arterial hypertension: comparison with bosentan and sildenafil. *Eur Respir J*. 2010;36:800–807.
  17. Henkens IR, Mouchaers KT, Vliegen HW, et al. Early changes in rat hearts with developing pulmonary arterial hypertension can be detected with three-dimensional electrocardiography. *Am J Physiol Heart Circ Physiol*. 2007;293:H1300–H1307.
  18. Galie N, Hoepfer MM, Humbert M, et al. Guidelines for the diagnosis and treatment of pulmonary hypertension: the task force for the diagnosis and treatment of pulmonary hypertension of the European Society of Cardiology (ESC) and the European Respiratory Society (ERS), endorsed by the International Society of Heart and Lung Transplantation (ISHLT). *Eur Heart J*. 2009;30:2493–2537.
  19. Iglarz M, Steiner P, Wanner D, et al. Vascular effects of endothelin receptor antagonists depends on their selectivity for ETA vs. ETB receptors and on the functionality of endothelial ETB receptors. *J Cardiovasc Pharmacol*. 2015. In press.
  20. Williams JH Jr, Bodell P, Hosseini S, et al. Haemodynamic sequelae of pulmonary fibrosis following intratracheal bleomycin in rats. *Cardiovasc Res*. 1992;26:401–408.
  21. Sato S, Kato S, Arisaka Y, et al. Changes in pulmonary hemodynamics during normoxia and hypoxia in awake rats treated with intratracheal bleomycin. *Tohoku J Exp Med*. 1993;169:233–244.
  22. Mutsaers SE, Foster ML, Chambers RC, et al. Increased endothelin-1 and its localization during the development of bleomycin-induced pulmonary fibrosis in rats. *Am J Respir Cell Mol Biol*. 1998;18:611–619.
  23. Park SH, Saleh D, Giaid A, et al. Increased endothelin-1 in bleomycin-induced pulmonary fibrosis and the effect of an endothelin receptor antagonist. *Am J Respir Crit Care Med*. 1997;156:600–608.
  24. Saleh D, Furukawa K, Tsao MS, et al. Elevated expression of endothelin-1 and endothelin-converting enzyme-1 in idiopathic pulmonary fibrosis: possible involvement of proinflammatory cytokines. *Am J Respir Cell Mol Biol*. 1997;16:187–193.
  25. Adamson IY, Bowden DH. The pathogenesis of bleomycin-induced pulmonary fibrosis in mice. *Am J Pathol*. 1974;77:185–197.
  26. Ryan J, Bloch K, Archer SL. Rodent models of pulmonary hypertension: harmonisation with the world health organisation's categorisation of human PH. *Int J Clin Pract Suppl*. 2011:15–34.
  27. Hess P, Clozel M, Clozel JP. Telemetry monitoring of pulmonary arterial pressure in freely moving rats. *J Appl Physiol (1985)*. 1996;81:1027–1032.
  28. Choudhary G, Troncales F, Martin D, et al. Bosentan attenuates right ventricular hypertrophy and fibrosis in normobaric hypoxia model of pulmonary hypertension. *J Heart Lung Transplant*. 2011;30:827–833.
  29. Rafikova O, Rafikov R, Kumar S, et al. Bosentan inhibits oxidative and nitrosative stress and rescues occlusive pulmonary hypertension. *Free Radic Biol Med*. 2013;56:28–43.
  30. Gatfield J, Mueller Grandjean C, Bur D, et al. Distinct ETA receptor binding mode of macitentan as determined by site directed mutagenesis. *PLoS One*. 2014;9:e107809.
  31. Kummer O, Haschke M, Hammann F, et al. Comparison of the dissolution and pharmacokinetic profiles of two galenic formulations of the endothelin receptor antagonist macitentan. *Eur J Pharm Sci*. 2009;38:384–388.
  32. Mauritz GJ, Kind T, Marcus JT, et al. Progressive changes in right ventricular geometric shortening and long-term survival in pulmonary arterial hypertension. *Chest*. 2012;141:935–943.
  33. To WS, Midwood KS. Plasma and cellular fibronectin: distinct and independent functions during tissue repair. *Fibrogenesis Tissue Repair*. 2011;4:21.
  34. Ho JE, Liu C, Lyass A, et al. Galectin-3, a marker of cardiac fibrosis, predicts incident heart failure in the community. *J Am Coll Cardiol*. 2012;60:1249–1256.
  35. Bjornstad JL, Neverdal NO, Vengen OA, et al. Alterations in circulating activin a, GDF-15, TGF-Beta3 and MMP-2, -3, and -9 during one year of left ventricular reverse remodelling in patients operated for severe aortic stenosis. *Eur J Heart Fail*. 2008;10:1201–1207.
  36. Yndestad A, Ueland T, Oie E, et al. Elevated levels of activin a in heart failure: potential role in myocardial remodeling. *Circulation*. 2004;109:1379–1385.
  37. Hashimoto O, Nakamura T, Shoji H, et al. A novel role of follistatin, an activin-binding protein, in the inhibition of activin action in rat pituitary cells. Endocytotic degradation of activin and its acceleration by follistatin associated with cell-surface heparan sulfate. *J Biol Chem*. 1997;272:13835–13842.
  38. Yndestad A, Larsen KO, Oie E, et al. Elevated levels of activin a in clinical and experimental pulmonary hypertension. *J Appl Physiol (1985)*. 2009;106:1356–1364.